Surface & Coatings Technology xxx (2016) xxx–xxx

Contents lists available at ScienceDirect

Surface & Coatings Technology

journal homepage: www.elsevier.com/locate/surfcoat

Improving corrosion stability of Zn—Al—Mg by alloying for protection of car bodies

Tomas Prosek [a,*], Andrej Nazarov [a], Frank Goodwin [b], Jan Šerák [c], Dominique Thierry [a]

[a] Institut de la Corrosion/French Corrosion Institute, 220 rue Pierre Rivoalon, 29200 Brest, France
[b] International Zinc Association, 2530 Meridian Parkway, Suite 115, Durham, NC 27713, USA
[c] University of Chemistry and Technology, Prague, Technická 5, 166 28 Praha 6, Czech Republic

ARTICLE INFO

Article history:
Received 21 December 2015
Revised 15 March 2016
Accepted in revised form 19 March 2016
Available online xxxx

Keywords:
Hot dip galvanizing
Alloy coatings
Atmospheric corrosion
Hem flange protection

ABSTRACT

Aluminium and magnesium are known for their ability to improve corrosion performance of zinc coatings used for steel protection in automotive applications. To investigate the inhibiting properties of other elements, series of model Zn—X, Zn—Al—X, Zn—Mg—X and Zn—Al—Mg—X alloys containing 0.2–2 wt% of titanium, mischmetal (mixture of cerium and other lanthanides), zirconium, molybdenum, chromium, boron, gallium, indium, copper, nickel, calcium, manganese and silicon were prepared and their corrosion performance in a cyclic accelerated test and at a marine field site and the ability to provide galvanic protection to steel in defects were characterized. On openly exposed surfaces, none of the investigated elements showed stronger inhibiting effect on atmospheric corrosion than Al and Mg. When exposed to marine climate, it was beneficial to combine Al and Mg. The corrosion stability of Zn—Al—Mg was further improved by addition of a fourth element. Quaternary Zn—Al—Mg—X alloys outperformed binary Zn—X and ternary Zn—Al—X and Zn—Mg—X alloys. In average, mass loss was 4-fold higher in confined zones simulating hem flanges. Strong inhibition with Mg and detrimental effects of Al on corrosion in confined zones was found. Several quaternary Zn—Al—Mg—X alloys with improved corrosion stability in both open and confined configurations were identified.

1. Introduction

Zinc-based coatings deposited by electroplating, hot-dip galvanizing and recently also by physical vapour deposition (PVD) are crucial for corrosion protection of steel. It is well known that manufacturing, mechanical and corrosion properties of zinc-based coatings can be improved by alloying. Besides established alloying elements such Al, Ni and Fe, magnesium was shown to provide a significant advantage when introduced to zinc. In earlier studies, additions of up to 1 wt% Mg were investigated with a rather modest effect on the corrosion stability [1–3]. Later on, hot-dip coatings containing from 1 to 3 wt% Mg in combination with Al were commercialised by Japanese and European steelmakers [4–11]. Zn—Mg coatings produced by PVD and containing about 16 wt% Mg in form of the $MgZn_2$ phase in the outer coating layer are under development [12–16]. Both Zn—Mg and Zn—Al—Mg provide improved corrosion stability when compared to traditional zinc coatings [4–20].

The rate of zinc corrosion under atmospheric weathering conditions is usually controlled by the rate of oxygen reduction [21]. It is affected by the composition and structure of the oxide layer covering the metal surface [22]. It was shown that oxygen adsorbs and reduces easily on surfaces covered with ZnO due to the rather good electrical conductivity of this oxide [11,16,23,24]. Modification of the oxide layer with alloying elements may reduce the electrical conductivity and improve the coating corrosion stability.

The aim of this study was to assess corrosion properties of a series of Zn—X, Zn—Mg—X, Zn—Al—X and Zn—Al—Mg—X model cast alloys in order to select compositions for potential application as hot-dip deposited galvanic coatings for protection of steel car bodies. It focuses on quaternary Zn—Al—Mg—X not yet investigated in a systematic way.

2. Selection of alloying elements

It is well known that aluminium and magnesium inhibit atmospheric corrosion of zinc. A number of other elements for Zn, Zn—Al, Zn—Mg and Zn—Al—Mg alloying were selected to assess their inhibition potential.

Zr and Ti species are used for conversion coating of zinc surfaces due to their ability to inhibit corrosion [9,25]. Ce has low electron work function similar to Mg and correspondingly low reversible potential of the formation of corrosion products [26]. Cerium oxide and hydroxide species can decrease the surface film potential, electron-emitting properties and efficiency of cathodic oxygen reduction. Zr and Ti create dielectric oxide films with high resistivity decreasing the electron transfer from the metal bulk to adsorbed oxygen molecules.

Cr and Mo improve self-passivation of many alloys and are incorporated in efficient zinc inhibitors and conversion coatings. Alloying of

* Corresponding author.
E-mail address: tomas.prosek@vscht.cz (T. Prosek).

http://dx.doi.org/10.1016/j.surfcoat.2016.03.062
0257-8972/

Table 1
Material denomination and composition measured by XRF.

Denomination	Chemical composition [wt%]				Denomination	Chemical composition [wt%]			
	Zn	Al	Mg	X		Zn	Al	Mg	X
Zn	>99.9				Zn—6Al—2In	92.1	5.6		1.9
Zn—2Ti	97.3			1.7	Zn—6Al—2Cu	91.8	6.3		1.6
Zn—2Mm	96.8			1.9	Zn—8Al—2Ni	89.9	7.7		2.0
Zn—2Zr	97.5			1.8	Zn—6Al—1Ca	92.4	5.7		1.4
Zn—0.01Mo	99.5			0.01	Zn—0.01Si	>99.9			<0.01
Zn—0.6Cr	99.0			0.6	Zn—2Mg—0.6Cr	97.5		2.0	0.6
Zn—0.0003B	99.3			0.0003	Zn—3Al—0.6Cr	96.4	3.0		0.6
Zn—2Ga	97.5			1.8	Zn—3Al—2Mg	94.9	3.0	2.1	
Zn—2In	97.7			1.8	Zn—3Al—2Mg—0.2Cr	94.6	3.1	2.1	0.2
Zn—2Cu	98.0			1.7	Zn—3Al—2Mg—0.5Cr	94.8	3.1	2.0	0.5
Zn—2Ni	97.1			2.5	Zn—3Al—2Mg—0.2Zr	94.7	3.0	2.1	0.2
Zn—1Ca	98.0			1.5	Zn—3Al—2Mg—0.6Zr	94.3	3.1	2.0	0.6
Zn—2Mg	97.8		2.0		Zn—3Al—2Mg—2Zr	93.2	2.9	2.0	1.9
Zn—7Mg	93.0		6.8		Zn—3Al—2Mg—0.2Ti	94.6	3.1	2.0	0.2
Zn—2Al	97.8	2.1			Zn—3Al—2Mg—0.6Ti	94.3	3.1	2.0	0.6
Zn—3Al	96.6	3.1			Zn—3Al—2Mg—2Ti	92.6	3.1	2.1	2.1
Zn—5Al	94.7	5.2			Zn—3Al—3Mg—0.3Mm[a]	93.6	3.0	3.1	0.3
Zn—7Mg—1Ti	92.4		6.8	0.6	Zn—3Al—2Mg—0.6Mm[a]	94.1	3.1	2.1	0.6
Zn—7Mg—1Mm[a]	91.2		7.2	1.2	Zn—3Al—2Mg—0.01Mo	94.8	3.1	2.1	0.01
Zn—7Mg—2Zr	90.5		7.5	1.8	Zn—3Al—2Mg—0.2Mn	94.8	2.9	2.1	0.2
Zn—7Mg—0.01Mo	93.0		6.7	0.01	Zn—3Al—2Mg—0.6Mn	94.2	3.1	2.1	0.6
Zn—7Mg—0.5Cr	92.9		6.6	0.5	Zn—3Al—2Mg—2Mn	92.8	3.1	2.1	1.9
Zn—7Mg—0.004B	92.0		7.3	0.004	Zn—3Al—2Mg—2Si	93.1	3.0	2.0	1.9
Zn—10Mg—2Ga	87.3		10.4	2.0	Zn—2Al—3Mg	95.0	1.9	3.0	
Zn—6Mg—2In	92.1		6.1	1.8	Zn—1Al—2Mg	96.7	1.1	2.2	
Zn—7Mg—2Cu	90.9		6.8	2.1	Zn—1Al—2Mg—2Si	94.8	0.9	2.1	2.1
Zn—7Mg—2Ni	91.1		6.5	2.2	Zn—2Al—2Mg	95.9	2.0	2.1	
Zn—7Mg—1Ca	92.2		6.5	1.1	Zn—2Al—2Mg—2Si	93.9	1.9	2.1	2.1
Zn—8Al—2Ti	89.4	8.3		2.0	Zn—5Al—2Mg	93.0	4.8	2.2	
Zn—9Al—2Mm[a]	89.0	8.6		1.6	Zn—5Al—2Mg—2Si	90.9	5.0	2.0	2.2
Zn—7Al—1Zr	92.0	6.7		1.1	Zn—3Al—2Mg—0.2Si	94.9	2.9	1.9	0.2
Zn—8Al—0.01Mo	92.1	7.6		0.01	Zn—3Al—2Mg—0.6Si	94.5	2.9	1.9	0.6
Zn—6Al—0.4Cr	93.0	6.3		0.4	Zn—3Al—2Mg—0.2Ca	94.9	3.0	1.9	0.2
Zn—6Al—0.0003B	93.3	6.0		0.0003	Zn—3Al—2Mg—0.6Ca	94.3	3.1	2.1	0.6
Zn—6Al—2Ga	92.1	5.8		2.0					

[a] Mm: Mischmetal, mixture of cerium and other lanthanides.

zinc-based coatings with Mo and Cr could decrease the anodic dissolution rate providing an eventual synergetic effect with elements acting as cathodic inhibitors such as magnesium [11,13,16,18,27].

Corrosion products forming in presence of Al^{3+} ions released at cathodes, layered double hydroxide (LDH), were proposed to be responsible for good corrosion stability of Al-alloyed zinc coatings by providing a barrier effect and reducing the oxygen reduction rate [5,7,11]. B, Ga, and In are trivalent metals that might form similar products or alter the structure of LDH by partly replacing Al^{3+}.

The amount of defects and electron carriers in oxide is affected by impurities as substitutional impurity changes the ionic charge at a lattice site. For example, substitution of zinc by copper, which would be probably present in the film as Cu^{+}, can compensate defects and reduce the amount of electrons available for charge transfer [21]. Such p-doping resulting from presence of e.g. Cu and Ni can decrease the conductivity and rate of cathodic processes on zinc oxide films.

Ca and Mg are low electron work function elements that can reduce the electron emitting properties by formation of mixed foreign oxide films. Electric conductivity of a surface film is governed by excitation of electrons across band gap, i.e. the transition of electrons from the top of the valence band to the bottom of the conductive band [3]. MgO and CaO have one of the highest band gaps of metal oxides of 7.7 and 6.9 eV, respectively [23].

3. Experimental

3.1. Materials

Three series of model cast alloys were prepared for this study. First, binary Zn—X and ternary Zn—Al—X and Zn—Mg—X alloys with target Al, Mg and X concentrations of 5, 6 and 2 wt% were prepared. Zn—5Al is a eutectic composition produced commercially. Zn—6Mg with the composition close to the Mg_2Zn_{11} phase showed the best corrosion stability from a number of Zn—Mg alloys containing 1–32 wt% Mg [27]. As X, Ti, Ce, Zr, Mo, Cr, Si, Mn, B, Ga, In, Cu, Ni and Ca were selected. Second, quaternary Zn—3Al—2Mg—X alloys were cast with the target concentration for X of 0.2, 0.6 and 2 wt%. Third, materials selected in view of expected good performance in confined zones modelling hem flanges with Al content varying from 1 to 5 wt% were made. A list of 69 cast materials is given in Table 1.

The model alloys were prepared by induction melting in a graphite crucible under argon protective atmosphere. Purity of raw Zn and Al was 99.99 wt%. It was at least 99 wt% for the other materials. After

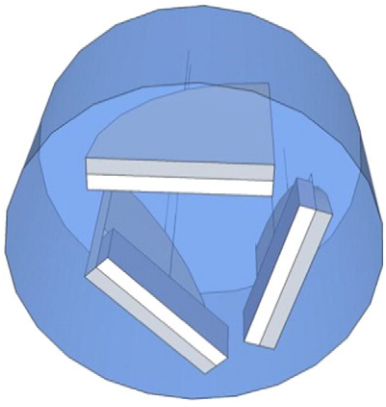

Fig. 1. Schematic drawing of steel/alloy couples for galvanic protection experiments.

Please cite this article as: T. Prosek, et al., Surf. Coat. Technol. (2016), http://dx.doi.org/10.1016/j.surfcoat.2016.03.062

Table 2
Ranking system for presence of red rust on steel in galvanic couples (alloy on top, steel in bottom).

Ranking	1	2	3
Description	No red rust	Slight red rusting	Heavy red rusting
Example			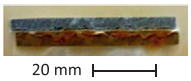

introduction to a crucible, raw materials were heat up to 500–800 °C depending on the composition and kept at the temperature for up to 6 h to dissolve and homogenize. Then, still under the protective atmosphere, the melt was poured into a brass mould. Cylindrical casts of 50 mm in diameter were cut to samples 2–4 mm thick. Before each experiment, they were polished down to 400 grit and their backsides masked with tape.

Microstructure of the alloys was studied after grinding, polishing and etching in Nital solution (10 vol% HNO_3 in methanol) by light and electron microscopy. Phase composition was analysed by X-ray diffraction (XRD) and energy dispersive X-ray spectroscopy (EDX). Chemical composition was measured by X-ray fluorescence (XRF). It is given in Table 1.

As reference, hot dip panels of Zn—0.2Al (Z; coating weight 275 g/m^2), Zn—5Al (ZA; 130 g/m^2), Zn—55Al—1.6Si (AZ; 150 g/m^2), Zn—1.5Al—1.5Mg (ZM; 190 g/m^2) and Zn—11Al—3Mg—0.2Si (ZMM; 100 g/m^2) were used. The panels were cut to 150 × 100 mm and backside and edges masked with tape.

3.2. Experimental procedure

ECC1 is a cyclic accelerated corrosion test developed and used by the automotive industry [28]. It is conducted at 35 °C and comprises humid (90% relative humidity, RH) and dry (55% RH) phases. Water solution containing 1 wt% NaCl acidified to pH 4 is sprayed over the samples during 30 min once a day. Four parallel samples of each composition were subjected to 42 daily cycles with total duration of six weeks.

Selected materials were exposed at a marine test site in Brest, France. The site is characterized by high corrosivity of C5 and C3 for steel and zinc, respectively, due to elevated chloride deposition of 1 g m^{-2} day^{-1} or higher. The typical average yearly temperature is 13 °C, RH 85% and time of wetness 500 h/month. Four replicates of 43 materials were exposed at 45° to horizontal facing south. Mass loss and corrosion depth were evaluated on two samples after 10 months and another two samples after 24 months of exposure.

Mass losses after the ECC1 test and field exposure were measured after removal of corrosion products in saturated water solution of glycine, NH_2CH_2COOH, at about 20 °C in an ultrasonic bath following the ISO 8407 standard [29]. For AZ, chromic acid (100 g/L CrO_3, 10 g/L $AgNO_3$) solution was used.

To assess the ability of model alloys to provide galvanic protection to steel, a piece of an alloy material with soldered wire was attached to a piece of similarly prepared carbon steel with a 120-μm thick insulating polymer membrane separating them. The exposed area was from 50 to 125 mm^2 with identical alloy to steel ratio 1:1. Schematic drawing of a galvanic sample is seen in Fig. 1.

Open circuit and galvanic potential of alloys and galvanic current flowing between carbon steel and alloy samples were measured in artificial rain water (852 mg/L Na_2SO_4, 4.3 mg/L $MgCl_2$, 3.1 mg/L $CaCl_2$, 8.9 mg/L NaCl, 10.5 mg/L NH_4NO_3). The composition was adapted from a study of He et al. [30] to reflect properties of rain water in inland Europe. It simulates low corrosive environments with low chloride concentration where alloyed materials might passivate. A galvanic couple was immersed in the solution for four weeks and electrochemical measurements were repeatedly performed. To assess the efficiency of galvanic protection, steel parts were inspected visually and ranked based on the amount of formed corrosion products (red rust). A simple ranking system from 1 to 3 is described in Table 2.

Because corrosion of hem flanges is critical for corrosion performance of car bodies, model hem flange samples of most cast materials were prepared. The sample design is seen in Fig. 2. The confined zone was formed with a glass slide fixed by double-coated tape. The confined zone opening had a width of 130 μm. It was systematically verified using a calibrated metal foil. The width (metal to glass) of the confined zone was 260 μm and size of the exposed metal was 28 × 20 mm. Other parts of the sample were masked with 130-μm vinyl tape. At least four parallel model hem flange samples for each material were exposed to ECC1 for six weeks. The confined zones were filled with the NaCl solution used for sample spraying prior the exposure to improve the test repeatability.

It needs to be noted that due to several factors, the results obtained using the sample design shown in Fig. 2 are only comparative. First, because of small sample size, the setup is not conforming to any standard and the kinetics of the occluded solution formation and corrosion processes are thus specific. Second, the typical duration of hem flange corrosion tests is twelve weeks, not six. Third, it was obviously impossible to assess the time to red rust appearance, which is one of the principal parameters to follow.

4. Results and discussion

4.1. Cyclic accelerated corrosion test

The ECC1 test was carried out separately for three series of cast alloys. Each time, selected alloys and a set of reference panels were

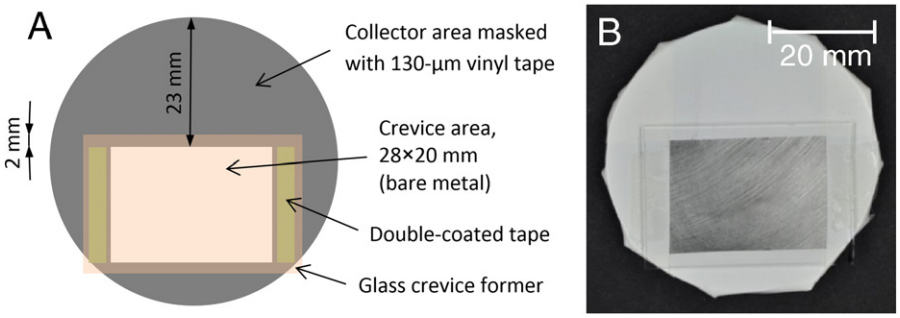

Fig. 2. Schematic drawing (A) and photograph (B) of a model hem flange sample; diameter 50 mm.

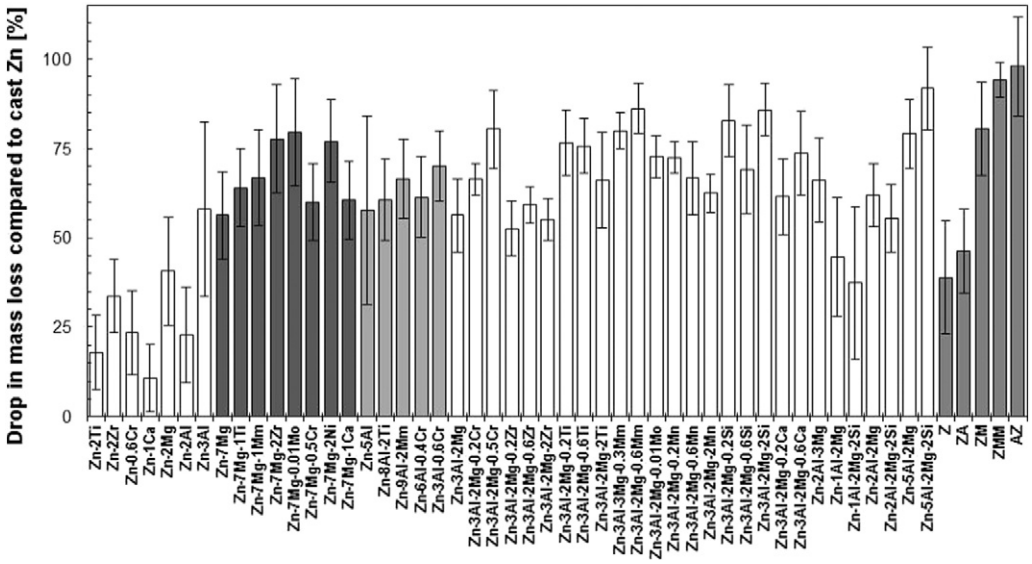

Fig. 3. Drop in mass loss of selected model alloys and reference materials compared to cast zinc after 6 weeks in ECC1.

exposed. Although the exposure conditions were apparently identical, there were differences in obtained mass losses in parallel tests. For example, mass loss of cast Zn with purity >99.9 wt% was 86 ± 8, 85 ± 6 and 67 ± 2 g m^{-2}. Thus, instead of absolute mass loss values, a relative drop in mass loss compared to that of cast zinc exposed in the same test was used as a measure of the effect of zinc alloying. The drop D expressed in % is defined by Eq. (1), where Δm stands for mass loss in g m^{-2}. Results are shown in Fig. 3. Only selected binary and ternary materials are displayed in sake of clarity.

$$D = \frac{\Delta m_{Zn} - \Delta m_{alloy}}{\Delta m_{Zn}} \quad (1)$$

Most reference panels showed about 2-fold lower mass loss than cast alloys with corresponding compositions. This may indicate the importance of the material microstructure, which is clearly different for coatings and for cast alloys [14,19,31–33]. It also suggests that the performance of the alloyed materials might further improve when applied as coatings.

In binary alloys, Mg and Al had the strongest inhibiting effect. Ti, Zr, Cr and Ca reduced mass loss of zinc by 11–34%. In Zn—Al—X and Zn—Mg—X ternary alloys, none of the third elements provided any substantial improvement in corrosion stability. Quaternary Zn—3Al—2Mg—X alloys outperformed the ternary ones providing 70% improvement to zinc in average.

The chart in Fig. 4 shows the effect of Al, Mg and Cr. Al and Mg improved the zinc corrosion stability in a similar extent and their effect was additive. This was reported earlier in conditions of another accelerated corrosion test [6]. The effect of chromium was low in ternary alloys with Mg. A stronger improvement was observed when combined with Al. Five-fold improvement in mass loss compared to Zn was observed for Zn—3Al—2Mg—0.5Cr.

Silicon provided very high inhibition efficiency in Zn—3Al—2Mg—2Si with seven-fold lower mass loss compared to Zn. It also improved corrosion stability of Zn—5Al—2Mg. Mass loss of Zn—5Al—2Mg—2Si was more than 10-fold lower than for cast zinc. Zn—1Al—2Mg—2Si and Zn—2Al—2Mg—2Si were more corroded than the base alloys. Except for Zn—2Mm, mischmetal (cerium) improved the stability of all alloys. It was particularly efficient in Zn—3Al—2Mg—Mm. The effect was strong already at 0.3 wt% Mm but further increased for Zn—3Al—2Mg—0.6Mm providing seven-fold improvement to Zn. Titanium was inhibiting corrosion of zinc but the effect in ternary alloys was low. In quaternary alloys, Ti seems to be most efficient at lower additions with the best stability demonstrated by Zn—3Al—2Mg—0.2Ti. Considering the very low solubility of molybdenum in zinc and the alloys, it showed surprisingly strong effect when combined with Mg or with Al and Mg. The effect of Mo addition to Zn and Zn—Al was negligible. The effect of manganese seems to be particularly advantageous at lower concentrations. Zn—3Al—2Mg—0.2Mn outperformed the materials with 0.6 and 2 wt% Mn. Alloying with other elements led to small improvements.

In summary, no binary or ternary alloys except of Zn—Mg, Zn—Al and Zn—Al—Mg showed particularly good results in the ECC1 test. Several quaternary Zn—Al—Mg—X alloys gave low mass loss.

4.2. Galvanic protection

To provide galvanic protection to steel at cut edges and in defects, the open circuit potential (E_{OC}) of a metallic coating must be sufficiently negative to that of steel. E_{OC} of the model alloys measured after 30 min of stabilization in artificial rain water was in a range from −1120 to −800 mV vs. saturated calomel electrode (SCE), i.e. safely negative to carbon steel above −600 mV vs. SCE. Since corrosion products can passivate the

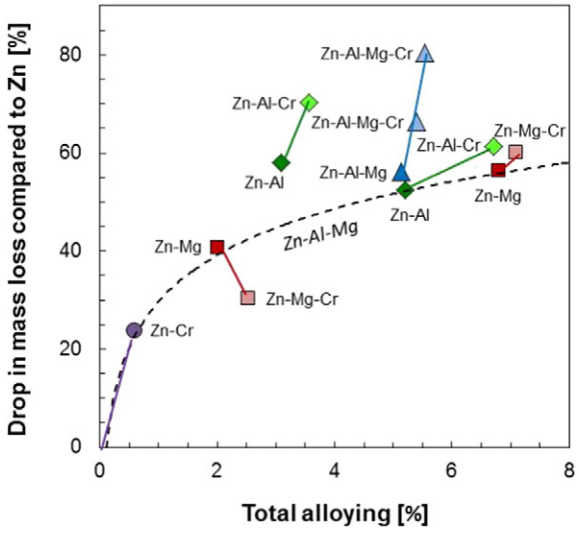

Fig. 4. Combined effect of alloying with Al and Mg (dashed curve) and Cr (full curves) on drop in mass loss compared to cast Zn after 6 weeks of exposure to ECC1.

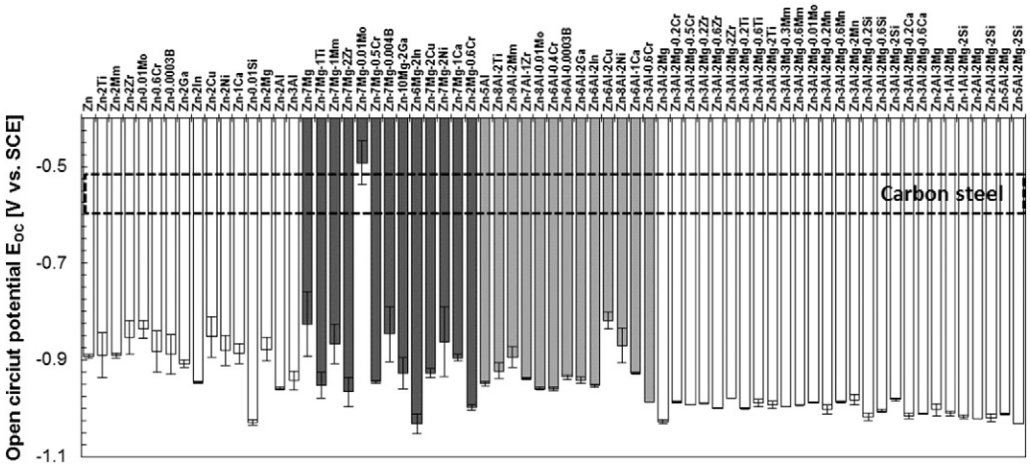

Fig. 5. Open circuit potential of model alloys after four weeks of exposure to artificial rain water; range of potentials of carbon steel is marked by dashed rectangle.

surface, galvanically coupled alloy-steel assemblies were kept in the environment for four weeks and E_{OC} re-measured 10 min after disconnection (Fig. 5). It moved by only 40 mV to more positive values in average. Except for Zn—7Mg—0.01Mo with E_{OC} increasing from −930 to −490 mV vs. SCE and becoming cathodic to steel, the alloys provided good galvanic protection to steel even in the low-aggressive electrolyte.

Galvanic current flowing between steel and alloy electrodes was measured by zero resistance ammetry (ZRA) 30 min after immersion. Most alloyed materials provided higher galvanic currents than 0.3 A m^{-2} for cast Zn. This was particularly true for Zn—Al—Mg(—X) alloys with 2-fold higher galvanic currents of 0.7 A m^{-2} in average. During four weeks of exposure, it dropped by an order of magnitude. Magnesium addition tended to lower the galvanic current, whereas aluminium increased it. The alloying with X had a limited effect.

Visual appearance of three parallel steel electrodes after four weeks of exposure to artificial rain water under galvanic protection was ranked using the system described in Table 2. Results are plotted in Fig. 6. Only four alloys protected steel from red rust formation to a lesser extent than cast Zn: Zn—2Ti, Zn—7Mg—1Mm, Zn—7Mg—0.01Mo and Zn—6Al—2Cu. Most alloys were more protective than Zn. The visual ranking principally agrees to the galvanic current measurements after four weeks of stabilization. Zn—Al—X alloys were more protective than Zn—Mg—X alloys and the binary Zn—X alloys ranked in between. Superior performance showed Zn—Al—Mg—X materials.

4.3. Field exposure

Mass loss of two replicate samples was measured after 10 months of exposure. Two more samples were assessed after 24 months of exposure. The latter data for all materials are given in Fig. 7 and both data sets for Zn—Al—Mg—X alloys are presented in Fig. 8.

Large difference in mass loss of cast Zn samples and reference line Z panels (Zn—0.2Al hot dip galvanized steel with masked edges) were observed after both 10 and 24 months of exposure. Since Z gave about similar mass loss as rolled zinc of 99.9% purity used for site calibration (8–17 g m^{-2} $year^{-1}$), the origin of this discrepancy cannot be the small amount of aluminium present in Z. No major impurities (<0.1 wt%) were found in the structure of the cast Zn samples by neither EDX nor XRF. The difference can be partly linked to sample geometry. The Z panels were about 7-fold larger than the cast Zn samples and edges of the former materials were masked.

When the reference panels are considered, mass loss of ZM alloyed with 1.5 wt% of Al and 1.5 wt% of Mg dropped by 40% compared to Z. It is in line with results of tests in similar environments carried out previously [20]. ZA outperformed ZM in both periods. It gave 3-fold lower mass loss than Z. The best results showed AZ with three- and four-times lower mass loss to Z after 10 and 24 months of exposure, respectively. It should be noted that a single panel of each reference material was available after 24 months of exposure. The relative error of measurement is expected to be similar as after 10 months when three replicates were assessed, i.e. about 7%.

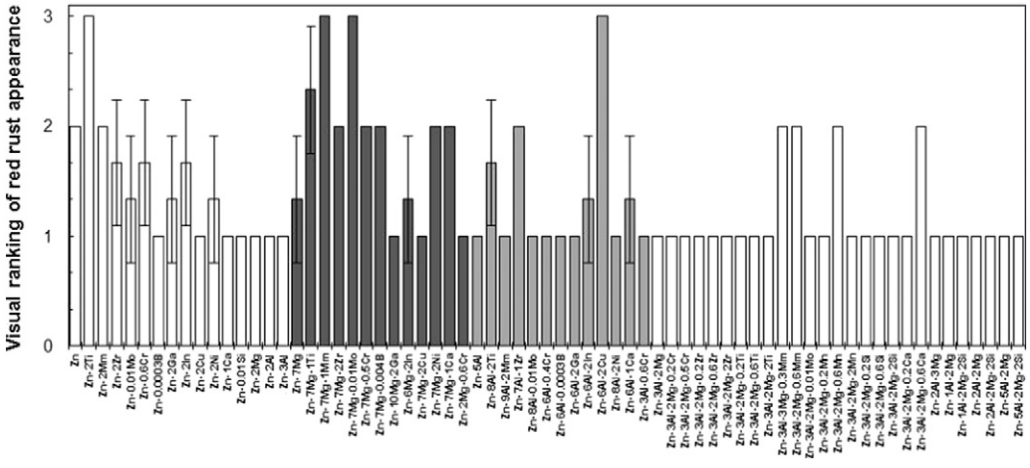

Fig. 6. Visual ranking of red rust appearance on steel electrodes after four weeks of galvanic coupling in artificial rain water; for the ranking system, see Table 2.

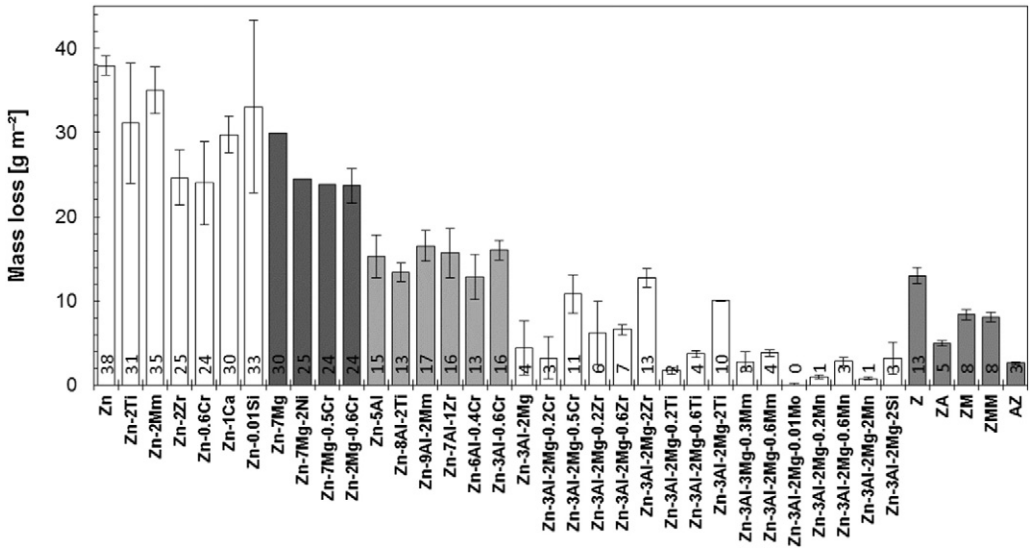

Fig. 7. Mass loss of model alloys and reference materials after 24 months of field exposure; standard deviations for reference materials are estimated based on 10-month data.

The difference between Z and the alloyed materials tended to increase with the exposure time, see Fig. 8. Mass losses between 10 and 24 months of exposure for Z, ZM and Zn—Al—Mg—X alloys increased by 100, 60 and 20% in average, respectively.

Binary Zn—X alloys with Zr and Cr were less corroded than Zn. Ti, Mm, Ca and Si showed only a minor inhibiting effect. In contrary to ECC1, mass loss of Zn—7Mg was only slightly lower than for Zn. Zn—5Al was the least corroded of all binary alloys. The inhibiting effect of aluminium in the marine climate was stronger than in conditions of the accelerated corrosion test, compare Fig. 3 and Fig. 8. It is observed regularly that cyclic accelerated corrosion tests tend to underestimate the corrosion stability of Al-containing coatings, both bare and painted [34]. This is most likely due to the lower stability of aluminium corrosion products under aggressive conditions where high pH levels are reached as a consequence of a high degree of acceleration [19]. All ternary Zn—Mg—X alloys were somewhat less corroded than Zn—7Mg but the difference was not large. No Zn—Al—X ternary alloy outperformed Zn—5Al.

Zn—3Al—2Mg and quaternary Zn—Al—Mg—X alloys showed the best corrosion stability. The lowest mass loss was observed for Zn—3Al—2Mg—0.01Mo and alloys containing Mn, see Fig. 8. Promising are also results for Zn—3Al—2Mg—0.2Cr, Zn—3Al—2Mg—0.2Ti, Zn—3Al—2Mg—0.6Ti, Zn—3Al—2Mg—0.3Mm, Zn—3Al—2Mg—0.6Mm and Zn—3Al—2Mg—2Si.

These results need to be considered in view of the experimental error of the pickling operation (removal of corrosion products) prior to mass loss measurements, which can reach 2–4 g m^{-2} for the small cast samples. Since most of the Zn—3Al—2Mg—X materials were highly resistant, any ranking within this group is only indicative. The experimental error is reflected in apparent drops in mass loss between months 10 and 24. Anyway, the data show on a strong synergy between Al and Mg in marine exposure conditions. Zn—7Mg and Zn—5Al were significantly more corroded than Zn—3Al—2Mg with a similar total content of alloying elements.

4.4. Corrosion in confined zones

The model hem flange panels displayed in Fig. 2 were exposed to ECC1 in three sets. Several alloys have been exposed repeatedly, e.g. Zn, each time with four replicates. Variation in mass loss between the tests was similar as for parallel samples in an identical test. E.g., mass losses measured for cast Zn were 178 ± 24, 225 ± 5 and 216 ± 73 g m^{-2} in three tests.

Mass losses in confined and open configurations under identical testing conditions for selected alloys are given in Fig. 9. The scatter for the confined configuration was larger than for open surfaces. It is observed regularly for this type of setup due to the importance of transport from and to the confined zone, which can be easily altered by e.g. blocking of the opening with corrosion products or minor variations in sample geometry.

For cast Zn and line Z, the mass loss increased by a factor of 2–3 in the confined zone. It is a rather typical value although it depends on exact geometry of a model hem flange setup and testing conditions [6, 20]. It shows that the setup was principally correct.

The alloys with magnesium provided the best performance of all binary alloys in the confined zone (Fig. 10A). They gave similar mass loss in both configurations showing on potentially exceptional resistance to perforation corrosion.

A dramatic increase in mass loss in the confined zone was measured for all binary alloys containing aluminium. It was 5- to 11-times higher than on the open surface. The inhibition due to Al alloying observed on

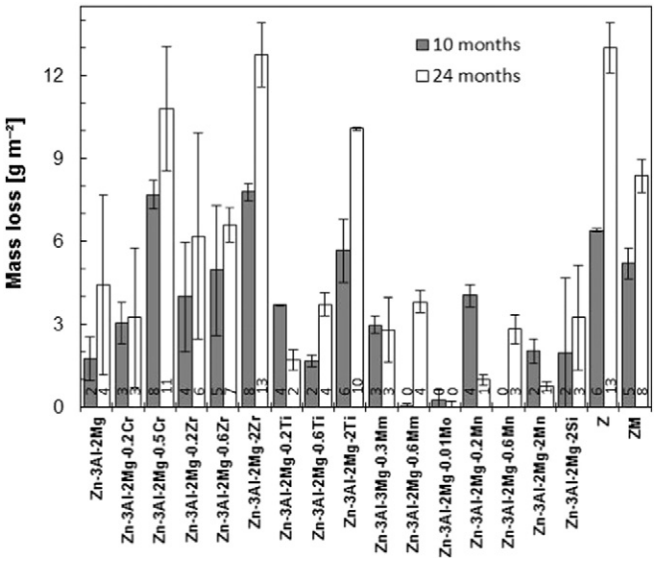

Fig. 8. Mass loss of Zn—Al—Mg—X model alloys and reference line panels of Z (Zn—0.2Al) and ZM (Zn—1.5Mg—1.5Al) after 10 and 24 months of exposure in marine climate.

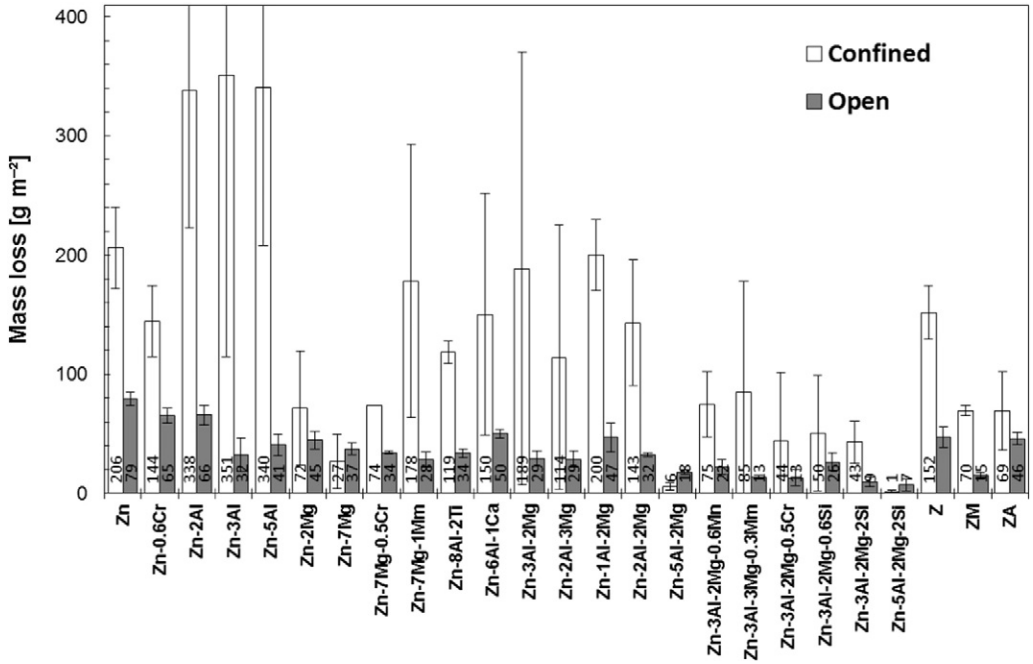

Fig. 9. Mass loss in confined and open configurations after 6 weeks of exposure to ECC1.

open surfaces fully disappeared in such sample geometry. A photograph of Zn—5Al after the 6-week exposure to ECC1 is shown in Fig. 10B.

The detrimental effect of aluminium and strong inhibition with magnesium may explain results of earlier model hem flange studies showing very good performance of Zn—Mg coatings prepared by PVD [13] and rather non-impressive results for Zn—Al—Mg coatings produced by hot dipping [6]. It is possible that the performance of the latter group of materials is negatively affected by the presence of aluminium. However, relatively good results for commercial ZA suggest that the unfavourable effect of aluminium does not need to be linked to any direct chemical role of Al-species in corrosion processes but rather to changing microstructure of the alloys [33]. ZA has a two-phase lamellar eutectic structure with no primary zinc dendrites in the outer coating layer [32]. The model Zn—Al alloys contained both primary zinc dendrites and the eutectics, which can be disadvantageous in view of formation of micro-galvanic cells and strong pH separation between cathodic and anodic sites [14,19].

On several Zn—Al—Mg alloys, it was tested whether the negative effect of aluminium on corrosion in the confined zone could be compensated by the Mg alloying. Results seem to suggest that whatever the Al to Mg mass ratio in a range from 1:2 to 3:2, the Zn—Al—Mg did not provide any particularly improved corrosion stability in model hem flanges, i.e. behaved closer to Zn and Zn—Al than to Zn—Mg. Ratios of confined- vs. open-situation mass losses varied from 4 to 8 for Zn—Al—Mg. Results for commercial ZM were basically in agreement. Mass loss of ZM increased in the confined zone close to 5-times compared to the openly exposed surface. Indeed, the line ZM was more protective than non-alloyed Z even in confined zones but the improvement factor dropped from 3 for the open to 2 for the confined configuration. Good performance in the model hem flange gave only Zn—5Al—2Mg with negligible mass loss.

To verify whether any alternative alloying element would have as strong inhibiting effect in the confined configuration as magnesium, a series of Zn—X materials were tested. With exception of chromium, none of X provided any improvement under such conditions. The confined vs. open mass loss ratio was in between 2 and 3 for all binary alloys.

It was examined if any element can further improve the performance of Zn—Mg or reduce the negative effect of Al. Both Zn—7Mg—0.5Cr and Zn—7Mg—1Mm were more corroded in the confined zone than Zn—7Mg. Most Zn—Al—X alloys were corroded similarly to Zn—5Al. Zn—8Al—2Ti and possibly Zn—6Al—1Ca performed better in the model hem flanges than Zn—Al alloys with the confined to open mass loss ratio of 3.5 and 3, respectively. However, the inhibition effect was weak compared to Mg.

Finally, it was investigated if any element can improve the corrosion stability of Zn—Al—Mg in confined zones. Due to very high scatter for eight samples of Zn—3Al—2Mg in two tests, the data are non-conclusive. It seems that most elements efficient in the open configuration were little inhibitive under conditions of limited transport. Promising results were obtained for Zn—3Al—2Mg alloyed with 0.6% Mn, 0.3% Mm and 0.5% Cr. The best performance showed repeatedly materials containing silicon. In particular, Zn—5Al—2Mg—2Si, Zn—2Al—2Mg—2Si,

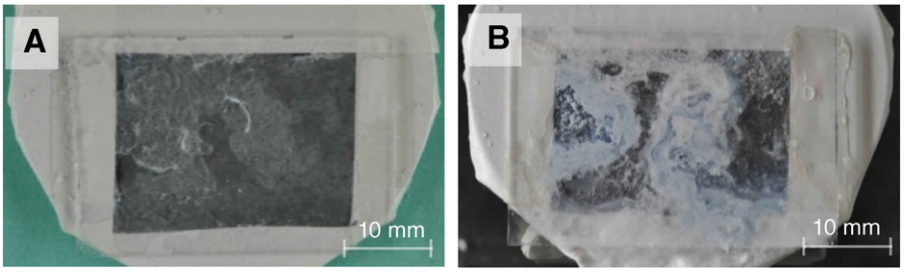

Fig. 10. Photographs of model hem flange samples of Zn—2Mg (A) and Zn—5Al (B) after 6 weeks in ECC1.

Please cite this article as: T. Prosek, et al., Surf. Coat. Technol. (2016), http://dx.doi.org/10.1016/j.surfcoat.2016.03.062

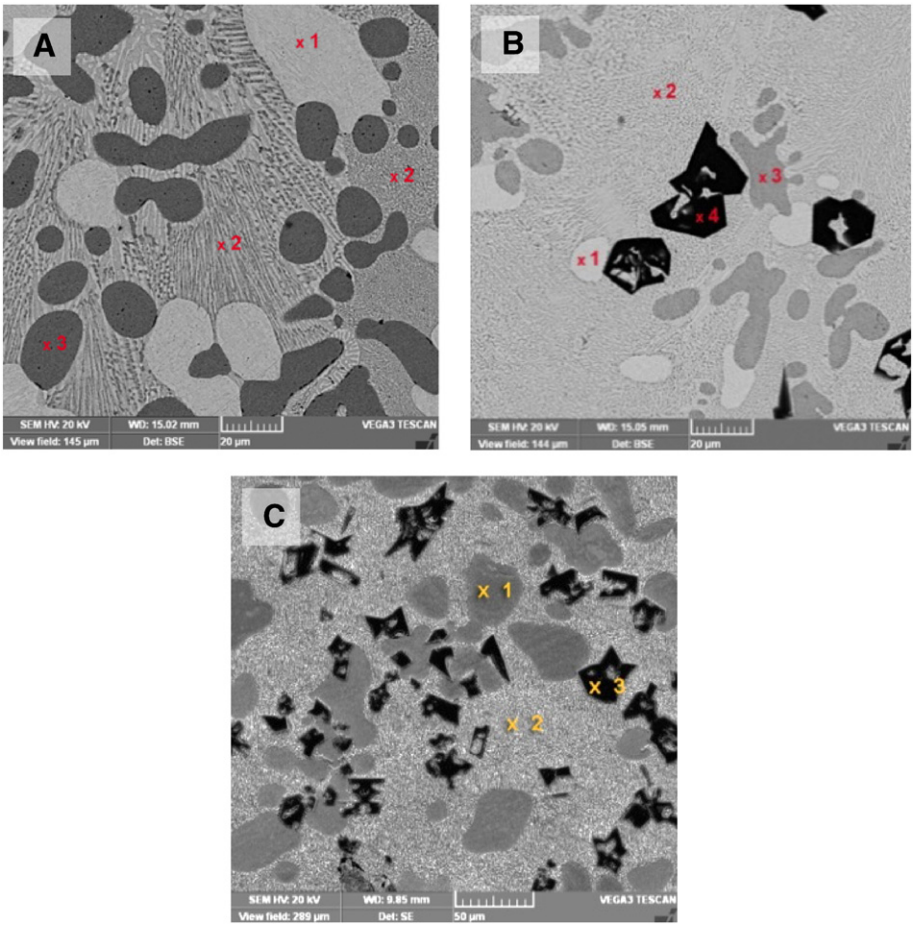

Fig. 11. Microstructure of Zn—5Al—2Mg (A), Zn—5Al—2Mg—2Si (B) and Zn—3Al—2Mg—2Si (C); 1: η-phase (Zn-rich), 2: Eutectics η-α-Mg_2Zn_{11}; 3: α-phase (Al rich); 4: Si particles.

Zn—3Al—2Mg—2Si and Zn—3Al—2Mg—0.6Si gave low mass losses in the model hem flanges. Visual appearance of these samples was also superior with a low amount of corrosion products.

Basic comparison of microstructures of more and less stable alloys suggests that those with a finer phase distribution tended to perform better. This can be shown for Si alloyed Zn—Al—Mg, see Fig. 11. Zn—Al—Mg—Si materials with a finer microstructure performed significantly better in both open and confined configurations. It can be linked to a lower acceleration of corrosion by local galvanic microcells and limited spatial pH variations. Improved performances of zinc-based coatings and alloys with finer microstructures in atmospheric exposure conditions were reported earlier [14,19,31,33].

The effect of alloying elements was thus different in open and confined configurations. There were elements inhibiting corrosion in both situation (in particular Mg, but – in a decreasing order – also Si, Cr, Mn and Ti) as well as those efficient only on open surfaces (Al) and, possibly, only in confined zones (Ca).

4.5. Material ranking

Improvements in corrosion stability provided by alloying compared to non-alloyed cast Zn in laboratory tests were weighted based on the expected importance of each test for material performance in service conditions. Similarly, outdoor performance relative to cast Zn was established by weighting the data obtained after 10 and 24 months.

Ten best performing cast materials in open and confined configurations in accelerated tests and in the open configuration at a marine test site are listed in Table 3. Several ternary Zn—Al—Mg alloys were highly corrosion resistant with the best results for Zn—5Al—2Mg. Only one more ternary alloy is in the list, Zn—7Mg—0.5Cr with a good stability in confined zones. From binary alloys, only Zn—2Mg and Zn—7Mg with superior stability in model hem flanges are included. It is well apparent that the best general corrosion stability provided quaternary Zn—Al—Mg—X alloys. Based on all three criteria, Zn—3Al—2Mg—2Si, Zn—5Al—2Mg—2Si and Zn—3Al—2Mg—0.5Cr can be considered most promising for further development.

Besides magnesium, strong inhibiting effect on corrosion in both open and confined geometries had only silicon. In this view, silicon is the most attractive alloying element of Zn—Al—Mg.

It was shown that small additions of Si, Cr, Ce (Mm), Mn, Mo and Ti can increase the corrosion stability of Zn—Al—Mg alloys, mostly at lower concentrations up to 0.6 wt%. It needs to be proved in further tests if the improvement is significant enough to be technically interesting in view of increased production complexity and costs.

The approach used in this study, i.e. rapid screening of a large number of model cast alloys, led to identification of compositions with

Table 3
Top-10 best performing materials ordered by decreasing corrosion resistance.

Open, laboratory	Open, field	Confined, laboratory
Zn—5Al—2Mg—2Si	Zn—3Al—2Mg—0.6Mn	Zn—5Al—2Mg—2Si
Zn—3Al—2Mg—2Si	Zn—3Al—2Mg—2Mn	Zn—5Al—2Mg
Zn—3Al—2Mg—0.5Cr	Zn—3Al—2Mg—0.01Mo	Zn—7Mg
Zn—3Al—2Mg—0.2Si	Zn—3Al—2Mg—0.2Ti	Zn—2Al—2Mg—2Si
Zn—5Al—2Mg	Zn—3Al—2Mg—0.6Mm	Zn—3Al—2Mg—2Si
Zn—3Al—2Mg—0.2Mn	Zn—3Al—3Mg—0.3Mm	Zn—3Al—2Mg—0.5Cr
Zn—3Al—2Mg—0.01Mo	Zn—3Al—2Mg—0.2Mn	Zn—3Al—2Mg—0.6Si
Zn—3Al—2Mg—0.2Ti	Zn—3Al—2Mg—0.2Cr	Zn—2Mg
Zn—3Al—2Mg—0.6Si	Zn—3Al—2Mg—0.6Ti	Zn—7Mg—0.5Cr
Zn—2Al—3Mg	Zn—3Al—2Mg	Zn—3Al—2Mg—0.6Mn

Please cite this article as: T. Prosek, et al., Surf. Coat. Technol. (2016), http://dx.doi.org/10.1016/j.surfcoat.2016.03.062

interesting anti-corrosion properties. However, there are limitations of this approach connected to different microstructures of cast alloys and coatings. Obviously, further investigations of steel panels coated with hot dip or other types of coatings with the identified compositions have to follow, taking into account also environmental, health, production cycle and galvanizing bath management issues. Certain compositions with superior corrosion stability may be of no industrial interest due to production limitations or formation of toxic or otherwise undesirable species during their production or exploitation.

5. Conclusions

- The corrosion stability of Zn—Al—Mg can be further improved by addition of a fourth element. In general, quaternary Zn—Al—Mg—X alloys outperformed binary Zn—X and ternary Zn—Al—X and Zn—Mg—X materials.
- Except for Zn—7Mg—0.01Mo, the alloys provided good galvanic protection to steel in defects. Zn—Al—X alloys were more protective than Zn—Mg—X. Superior galvanic protection potential was revealed for Zn—Al—Mg—X.
- Strong inhibition with Mg and detrimental effect of Al in confined zones simulating hem flanges was found. Comparison to reference hot-dip materials suggests that the detrimental effect of aluminium was linked more to coarser microstructures leading to formation of micro-galvanic cells and spatial pH separation between anodic and cathodic sites than to changes in the electrolyte chemistry. Alloying of Zn—Al—Mg with silicon inhibited corrosion in confined zones. It was probably due to a finer phase distribution.
- Materials with promising anti-corrosion properties under multiple exposure conditions with application potential for steel galvanizing for protection of car bodies were identified.

Acknowledgements

All members of the Galvanized Autobody Partnership program are thanked for their valuable inputs. We wish to thank Cecile Hall, Anne Le Gac and Vanessa Le Vern of Institut de la Corrosion for technical assistance with the corrosion experiments and Jan Stoulil of the University of Chemistry and Technology in Prague for conducting a part of the electrochemical experiments.

References

[1] H.E. Townsend, On the effects of magnesium on the atmospheric corrosion resistance of galvanized sheet steel, Corrosion 44 (1988) 229–230.
[2] C. Dagbert, R. Boulif, J. Galland, C. Cabrillac, Effect of galvanizing bath additives on atmospheric corrosion resistance of galvanized steels, Mater. Tech. 78 (1990) 11–16.
[3] X.G. Zhang, Corrosion and electrochemistry of zinc, Plenum Press, New York, 1996.
[4] K. Nishimura, H. Shindo, K. Kato, Y. Morimoto, Microstructure and corrosion behaviour of Zn—Mg—Al hot dip galvanized steel sheet, Proc. of Galvatech '98, Chiba, Japan 1998, pp. 437–442.
[5] S. Schürz, M. Fleischanderl, G.H. Luckeneder, K. Preis, T. Haunschmied, G. Mori, A.C. Kneissl, Corrosion behaviour of Zn—Al—Mg coated steel sheet in sodium chloride-containing environment, Corros. Sci. 51 (2009) 2355–2363.
[6] T. Prosek, N. Larché, M. Vlot, F. Goodwin, D. Thierry, Corrosion performance of Zn—Al—Mg coatings in open and confined zones in conditions simulating automotive applications, Mater. Corros. 60 (2010) 412–420.
[7] P. Volovitch, T.N. Vu, C. Allély, A. Abdel Aal, K. Ogle, Understanding corrosion via corrosion product characterization: II. Role of alloying elements in improving the corrosion resistance of Zn–Al–Mg coatings on steel, Corros. Sci. 53 (2011) 2437–2445.
[8] B.J. Goo, B.R. Lee, M.B. Moon, S.J. Oh, Corrosion properties of Zn alloy coated steel sheet for automotive panels, Proc. of 19th International Corrosion Congress, Jeju, Korea, 2014.
[9] T. Lostak, A. Maljusch, B. Klink, S. Krebs, M. Kimpel, J. Flock, S. Schulz, W. Schuhmann, Zr-based conversion layer on Zn—Al—Mg alloy coated steel sheets: insights into the formation mechanism, Electrochim. Acta 137 (2014) 65–74.
[10] J. Duchoslav, R. Steinberger, M. Arndt, T. Keppert, G. Luckeneder, K.H. Stellnberger, J. Hagler, G. Angeli, C.K. Riener, D. Stifter, Evolution of the surface chemistry of hot dip galvanized Zn—Mg—Al and Zn coatings on steel during short term exposure to sodium chloride containing environments, Corros. Sci. 91 (2015) 311–320.
[11] M. Salgueiro Azevedo, C. Allély, K. Ogle, P. Volovitch, Corrosion mechanisms of Zn(Mg,Al) coated steel: 2. The effect of Mg and Al alloying on the formation and properties of corrosion products in different electrolytes, Corros. Sci. 90 (2015) 482–490.
[12] T. Koll, K. Ullrich, J. Faderl, J. Hagler, A. Spalek, Properties and potential applications of ZnMg-alloy-coatings on steel sheet by PVD, Proc. of Galvatech '04, Chicago, IL, United States 2004, pp. 803–812.
[13] N.C. Hosking, M.A. Strom, P.H. Shipway, C.D. Rudd, Corrosion resistance of zinc—magnesium coated steel, Corros. Sci. 49 (2007) 3669–3695.
[14] R. Krieg, A. Vimalanandan, M. Rohwerder, Corrosion of zinc and Zn–Mg alloys with varying microstructures and magnesium contents, J. Electrochem. Soc. 161 (2014) C156–C161.
[15] T. Prosek, D. Persson, J. Stoulil, D. Thierry, Composition of corrosion products formed on Zn—Mg, Zn—Al and Zn–Al–Mg coatings in model atmospheric conditions, Corros. Sci. 86 (2014) 231–238.
[16] J. Stoulil, T. Prosek, A. Nazarov, J. Oswald, P. Kriz, D. Thierry, Electrochemical properties of corrosion products on Zn—Al–Mg based coatings, Mater. Corros. 66 (2015) 777–782.
[17] D. Persson, D. Thierry, N. LeBozec, T. Prosek, In situ infrared reflection spectroscopy studies of the initial atmospheric corrosion of Zn–Al–Mg coated steel, Corros. Sci. 72 (2013) 54–63.
[18] J. Sullivan, N. Cooze, C. Gallagher, T. Lewis, T. Prosek, D. Thierry, In-situ monitoring of corrosion mechanisms and phosphate inhibitor surface deposition during corrosion of zinc—magnesium–aluminium (ZMA) alloys using novel time-lapse microscopy, Faraday Discuss. 180 (2015) 361–379.
[19] A. Vimalanandan, A. Bashir, M. Rohwerder, Zn—Mg and Zn—Mg–Al alloys for improved corrosion protection of steel: Some new aspects, Mater. Corros. 65 (2014) 392–400.
[20] N. LeBozec, D. Thierry, A. Peltola, L. Luxem, G. Luckeneder, G. Marchiaro, M. Rohwerder, Corrosion performance of Zn—Mg–Al coated steel in accelerated corrosion tests used in the automotive industry and field exposures, Mater. Corros. 64 (2013) 969–978.
[21] L. Rosenfeld, Atmospheric corrosion of metals. Some questions of theory, Proc. of 1st International Congress on Metallic Corrosion, London 1961, pp. 243–253.
[22] C. Deslouis, M. Duprat, C. Tulet-Tournillon, The cathodic mass transport process during zinc corrosion in neutral aerated sodium sulphate solutions, J. Electroanal. Chem. 181 (1984) 119–136.
[23] V.E. Henrich, P.A. Cox, The surface science of metal oxides, Cambridge University Press, 2000.
[24] A.L. Rudd, C.B. Breslin, Photo-induced dissolution of zinc in alkaline solutions, Electrochim. Acta 45 (2000) 1571–1579.
[25] S. Verdier, N. van der Laak, F. Dalard, J. Metson, S. Delalande, An electrochemical and SEM study of the mechanism of formation, morphology, and composition of titanium or zirconium fluoride-based coatings, Surf. Coat. Technol. 200 (2006) 2955–2964.
[26] J. Hölzl, F.K. Schulte, Work function of metals, Solid Surface Physics, Springer-Verlag, Berlin Heidelberg New York 1979, p. 9.
[27] T. Prosek, A. Nazarov, U. Bexell, D. Thierry, J. Serak, Corrosion mechanism of model zinc—magnesium alloys in atmospheric conditions, Corros. Sci. 50 (2008) 2216–2231.
[28] Test method D17 2028, Corrosion test by automatic change of phases of salt spray, drying and humidity (ECC1), Standardisation of Renault Automobiles, DMI/Service 65810, 2007.
[29] ISO 8407, Corrosion of metals and alloys, Removal of Corrosion Products From Corrosion Test Specimens, 2009.
[30] W. He, I. Odnevall Wallinder, C. Leygraf, A comparison between corrosion rates and runoff rates from new and aged copper and zinc as roofing material, Water Air Soil Pollut. 1 (2001) 67–82.
[31] J. Elvins, J.A. Spittle, Microstructural changes in zinc aluminium alloy galvanising as a function of processing parameters and their influence on corrosion, Corros. Sci. 47 (2005) 2740–2759.
[32] J. Elvins, J.A. Spittle, J.H. Sullivan, D.A. Worsley, The effect of magnesium additions on the microstructure and cut edge corrosion resistance of zinc aluminium alloy galvanised steel, Corros. Sci. 50 (2008) 1650–1658.
[33] T. Prosek, J. Hagström, D. Persson, N. Fuertes, F. Lindberg, O. Chocholaty, C. Taxén, J. Serak, D. Thierry, Effect of the microstructure of Zn–Al and Zn–Al–Mg model alloys on corrosion stability, sent for publication in Corros. Sci.
[34] T. Prosek, A. Nazarov, A. Le Gac, D. Thierry, Coil-coated Zn–Mg and Zn–Al–Mg: effect of climatic parameters on the corrosion at cut edges, Prog. Org. Coat. 83 (2015) 26–35.

Please cite this article as: T. Prosek, et al., Surf. Coat. Technol. (2016), http://dx.doi.org/10.1016/j.surfcoat.2016.03.062